A ^{18}F-MPPF PET Normative Database of 5-HT$_{1A}$ Receptor Binding in Men and Women Over Aging

Nicolas Costes, MSc[1,2]; Isabelle Merlet, PhD[3,4]; Karine Ostrowsky, MD[3]; Isabelle Faillenot, PhD[5]; Franck Lavenne, BSc[1,4]; Luc Zimmer, PharmD, PhD[1,6]; Philippe Ryvlin, MD, PhD[3,6]; and Didier Le Bars, PharmD, PhD[1,6]

[1]Imagerie du vivant, PET Centre, Centre d'Etude et de Recherche Multimodales et Pluridisciplinaires, Lyon, France; [2]Centre Nationale de la Recherche Scientifique, Paris, France; [3]Équipe d'Accueil 1880, Neurological Hospital, Lyon, France; [4]Institut National de la Santé et de la Recherche Médicale, Paris, France; [5]Institut Fédératif des Neurosciences de Lyon, Lyon, France; and [6]Université Claude Bernard de Lyon, Lyon, France

Neurotransmission imaging studies require normative data for the statistical assessment of neurophysiologic dysfunctions. 2′-Methoxyphenyl-(*N*-2′-pyridinyl)-*p*-^{18}F-fluoro-benzamidoethylpiperazine (^{18}F-MPPF) is a specific serotonin 5-HT$_{1A}$ antagonist PET tracer recently characterized, modeled, and used for clinical research to explore abnormalities in the serotoninergic system. Our study reports, to our knowledge, the first large normative imaging database of ^{18}F-MPPF binding potential (BP) over aging, for both males and females. **Methods:** Fifty-three healthy volunteers (27 females, 26 males; age, 20–70 y) were selected to undergo structural MRI and single-injection ^{18}F-MPPF multiframe dynamic PET. ^{18}F-MPPF BP values were computed using a nonlinear modeling method with tissue reference. The statistical assessment of the effect of age and sex was performed both at the anatomic structure level, using regions of interest drawn manually on individual MR images, and at the voxel level, using normalized BP parametric images in different statistical parametric mapping designs. **Results:** A negative linear correlation between age and ^{18}F-MPPF binding (3.6% decrease by decade) was found in females but not in males and involved most of the limbic and paralimbic regions; on the other hand, males in their 30s showed decreased binding in most cerebral regions. **Conclusion:** A comparison of males and females revealed higher BP values independent of age in females in the right hemisphere and a different evolution of BP over aging. These results confirm the necessity of a database for further statistical analysis in individuals or groups with pathology.

Key Words: PET; ligand; serotonin receptors; 5-HT$_{1A}$; database

J Nucl Med 2005; 46:1980–1989

In the mammalian nervous system, serotonin (5-HT) mediates a large variety of physiologic responses (development, pain, sleep, mood, eating, memory, attention), behaviors (stress, aggression, panic, sexual behavior), or neuropsychiatric problems (depression, sleep disturbance, eating disorders, anxiety, suicide, schizophrenia, obsessive compulsive disorder) through one of the widest range of receptors known for any neurotransmitter (*1*). Most of these receptors have been characterized; yet, to date, the 5-HT$_{1A}$ subtype remains the best known in terms of structure, pharmacology, and action.

The recent development of selective PET ligands for 5-HT receptors permits the in vivo exploration of the serotoninergic system in humans (*2*). In particular, two specific radioligands for 5-HT$_{1A}$ receptors have been used with PET. The first to be developed, ^{11}C-WAY100635, is a high-affinity selective antagonist of 5-HT$_{1A}$ receptors. Binding site extension was delineated (*3*) and quantified (*4*). These studies confirmed that 5-HT$_{1A}$ receptors are mainly located in the limbic areas and in the raphe nuclei but are also present in the paralimbic and neocortical regions.

The fluoro analog 2′-methoxyphenyl-(*N*-2′-pyridinyl)-*p*-^{18}F-fluoro-benzamidoethylpiperazine (^{18}F-MPPF) was synthesized shortly after (*5*) and, when compared with ^{11}C-WAY100635, offers an affinity more similar to that of 5-HT for 5-HT$_{1A}$ receptors (inhibition constant = 3.3 nmol/L) (*6*) and a longer half-life (107 min). In vivo and ex vivo distribution studies in rat (*7*), cat (*5,8*), and humans (*9*) confirmed the selective binding of the molecule in cerebral regions rich in 5-HT$_{1A}$ receptors, such as the dorsal raphe nuclei, the limbic and paralimbic regions, and, with less intensity, the neocortex. Quantification studies using a 3-compartmental simplified reference tissue model (SRTM) confirmed that binding potential (BP) values were correlated with the maximum number of available binding sites

Received Feb. 14, 2005; revision accepted Aug. 1, 2005.
For correspondence or reprints contact: Nicolas Costes, MSc, CERMEP, 59 boulevard Pinel, 69677 Bron Cedex, France.
E-mail: costes@cermep.fr

(B_{max}) and, therefore, could be considered as a reliable index of local receptor concentration (*10*).

Although these studies emphasized the potential use of both ligands for quantitative studies of the serotoninergic 5-HT_{1A} system in vivo, small groups of subjects were examined, which lead to a rather high variability of BP values. Certainly, significant variations in the quantification of 5-HT_{1A} receptor binding have been described previously using ^{11}C-WAY100635 (*11–13*). These variations were observed especially in small structures, such as the raphe nuclei or the amygdala, which are of particular interest for the study of neurologic diseases.

The aim of our study was to obtain data for ^{18}F-MPPF PET in a large group of healthy subjects (males and females) to test for the possible influence of age and sex on the variability of ^{18}F-MPPF PET BP. Moreover, our goal was also to provide a large control database appropriate for statistical parametric mapping (SPM) to ^{18}F-MPPF PET studies in 5-HT–related neuropsychiatric disorders (such as depression, eating disorders, Alzheimer, migraine or epilepsy) in which patients of wide age range or of specific sex are recruited.

MATERIALS AND METHODS

Subjects

Fifty-three healthy subjects (26 males [mean age ± SD, 41.7 ± 13.5 y; range, 20–68 y] and 27 females [mean age ± SD, 41.7 ± 14.1 y; range, 19–70 y]) were selected to participate in the study. Male and female control subjects were recruited to obtain a homogeneous age distribution between 19 and 70 y, with approximately 6 male and 6 female subjects for each decade of age. Subjects gave their written consent to participate in the study, which was approved by the local ethical committee (Centre Léon Bérard, Lyon, France) in accordance with the Helsinki Declaration and French rules protecting persons. Subjects were interviewed by a medical doctor to verify that they did not meet any of the following exclusion criteria: (i) sign or history of neurologic, psychiatric, cardiovascular, pleuro-pulmonary or hematologic disease; (ii) ongoing neuroleptic, antiparkinsonian α-methyl-dopa, β-blocker, MAOI-A or -B (MAOI = monoamine oxidase inhibitor), tricyclic antidepressant, or thymoregulator treatment; (iii) pregnancy; (iv) hormone replacement therapy; (v) consumption of recreational drugs (canabis, exctasy); (vi) contraindication to MRI; (vii) brain MRI lesion. Moreover, each subject was asked for his or her consumption of tobacco or alcohol. Heavy consumers of alcohol or tobacco were excluded. Five subjects smoking <10 cigarettes/d and 9 subjects taking 1–2 wine glass units/d (1 wine glass unit = 125 mL of wine according to the Medical Council of Alcohol) were included in the study. Second, all subjects were evaluated for depression using the General Health Questionnaire (GHQ-28) by Goldberg and Hillier (*14*). Only subjects with a score below the threshold for depression (<7) were included in the study.

MRI

A 3-dimensional multiplanar reconstruction anatomic MRI scan was performed on each subject, yielding a volume of 130–170 slices with cubic voxels of 1 mm^3 with 256 × 256 voxels in each transverse plane.

PET Scan of ^{18}F-MPPF

The methodology of tracer production, scan acquisition, and data processing has been described previously (*15,16*). Briefly, ^{18}F-MPPF was acquired in 35 frames with a CTI Exact HR+ scanner for 60 min after the injection of 153–250 MBq of ^{18}F-MPPF (mean ± SD, 192.7 ± 23.8 MBq). Sinograms were normalized, attenuated, and scatter corrected and then subsequently reconstructed with filtered backprojection (Hanning filter: cutoff, 0.5 cycle/voxel). This yielded to a dynamic study of 35 volumes of 128 × 128 × 63 with a voxel size of 2.04 × 2.04 × 2.42 mm^3. The binding parameters of the tracer were estimated according to the 3-compartment SRTM previously applied to ^{11}C-WAY100635 (*17*). This model is based on the analytic solution of the compartment model that is used to estimate 3 parameters without the use of an arterial sampling input function: R_1 (ratio of plasma to brain transport constant in the region of interest [ROI] and in the reference region), k_2 (tracer's efflux in the vascular system), and BP (ratio of available receptor density to receptor affinity, $BP = B_{max}/K_d$, where K_d is the dissociation constant). The cerebellum was taken as the reference region. The SRTM has been evaluated with a correlation study between parameters obtained with a complete nonlinear 3-compartement model (*10*) and the SRTM BP calculated in 20 ROIs.

The images were processed with the SRTM 2 different ways: one based on mean ROI activity curves (ROI analysis) and the other based on voxel level and SPM (parametric image analysis).

ROI Analysis. Individual ^{18}F-MPPF static images (summed from 0 to 60 min) were resliced in a transverse orientation parallel to the bihippocampal plane to optimally outline the mesial and lateral temporal regions. The same rotation parameters were applied to the dynamic acquisition. Independently, the MR image was coregistered with the ^{18}F-MPPF static image by an automated method based on Mutual Information criteria (SPM; Welcome Department of Cognitive Neurology, London, U.K.). Anatomic ROIs were manually drawn on the coregistered MR image by one of the authors. Four hundred ROIs were drawn and regrouped into anatomic volumes of interest (VOIs) to describe left and right amygdala, hippocampi, parahippocampal gyri, temporal poles, insula, anterior and posterior cingulate gyri, orbitofrontal cortices, inferior, middle, and superior temporal gyri, subcentral operculi, inferior and superior parietal lobules, frontal and occipital cortices, and thalami. As raphe nuclei cannot be identified on MRI, this region was outlined directly on the static ^{18}F-MPPF image by thresholding the activity at 80% of the local maximum in the brainstem. This region was a posteriori visualized on the MR image to check for its proper location in the periacqueductal gray matter. All ROIs were then applied to dynamic PET to extract time–activity curves and to obtain mean regional values of R_1, k_2, and BP for each ROI.

Parametric Image Analysis. For each subject, the MR image was coregistered with the static PET image in its acquisition orientation. On the coregistered MR image, a large ROI was outlined in the cerebellum and was used as a unique reference region for the simplified model applied to each voxel. From individual voxel time–activity curves, the parametric images of R_1, k_2, and BP were determined. Individual parametric images were then transformed into a standard space using the nonlinear transformation matrix derived from the spatial normalization of the individual's MR image to the T1 MRI default template (MNI template of the ICBM Project), and smoothed using an 8 × 8 × 8 mm^3 full width at half maximum isotropic gaussian kernel that

takes into account interindividual anatomy variability and improves the sensitivity of the statistical analysis.

Statistical Inference. For the ROI analysis, 2 separate statistical analyses for men and women were performed on mean regional BP values considered as independent measures.

First, we performed a linear regression of BP with age for each anatomic ROI with left and right BP values averaged. The r^2 coefficient was taken as the index of correlation with a standard Fisher z-score and P for significant assessment. To evaluate the impact of partial-volume effect (PVE) on BP values, we calculated a linear regression of BP versus ROI volumes.

We then performed an ANOVA for each anatomic ROI using laterality (left and right hemisphere) as an independent factor and the decade of age (20s, 30s, 40s, 50s, and 60s) as a group factor.

SPM99 was used for the voxel-based analysis on the normalized smoothed parametric BP images of the 53 control subjects. Three linear models were used to assess the variability due to sex or age between groups. In analysis I, we applied a 2-sample t test between males and females with individual BP values taken as covariates for interindividual adjustment. In analysis II, the design was an analysis of covariance (ANCOVA) with age considered as a covariate, sex as a group factor, and individual global BP values taken as covariates for interindividual adjustment. To perform analysis III, we used an ANOVA with sex and decade of age as group factors and individual global BP as a covariate for adjustment. Statistical parametric maps of the t statistic (SPM$\{t\}$) were calculated with a threshold of $P = 0.001$ uncorrected at the voxel level. Significant clusters were selected at a corrected cluster level of $P < 0.05$ determined from a joint probability of peak height and cluster size (*18*).

RESULTS

Relationship Between BP and ROI Volumes

No significant correlation between BP and ROI volumes was found for any regions except in the right insula ($P < 0.04$) of females and in the raphe nuclei ($P < 0.035$) of males. However, in these regions, BP variations were inversely correlated with ROI volumes.

Normative Data for ROI Analysis

Table 1 reports BP values for 18 anatomic regions in men and women. As there was no significant difference between left and right BP, the left and right values were mixed to determine the mean BP and the SD in each ROI for each decade of age. Minimal BP values were found in the thalamus and maxima in the hippocampus, with a highest mean of 1.27 ± 0.07 for women in their 30s and 1.28 ± 0.12 for men in their 20s. Minima were found in women in their 60s and in the males in their 30s. BP mean values ranged between 0.5 and 1.2 in limbic areas, between 0.5 and 0.6 in the lateral temporal cortex, between 0.3 and 0.6 in other neocortical regions, and between 0.3 ± 0.1 and 0.6 ± 0.1 in the raphe nuclei. Scatter plots of BP values versus age are illustrated in Figure 1 for all 18 ROIs.

Sex Difference in ^{18}F-MPPF Binding

For the SPM analysis I, the unpaired t test comparing BP images in males and females did not reveal any difference in ^{18}F-MPPF binding. However, when considering age as a covariate (analysis II), BP appeared significantly greater for women in several areas located in the limbic, paralimbic, and frontal regions (Table 2; Fig. 2A). The size of significant clusters was bigger in the right than in the left hemisphere (Fig. 2B). For men, BP was significantly greater in a single cluster, which appeared to be related to a side effect due to the normalization procedure (Fig. 2C).

Linear Variation of BP with Age

Females. The SPM analysis II, exploring the linear regression between age and ^{18}F-MPPF binding, showed a significant BP decrease with age involving most cortical areas (Fig. 2D). The most significantly correlated areas were found in the superior and middle temporal gyri bilaterally, the left middle frontal gyrus, the insula, the temporooccipital region, and the cingulate gyrus (Table 3; Fig. 2E), sparing only the left amygdala and the orbitofrontal cortex. The inverse contrast did not reveal any significant BP increase.

The ROI analysis, illustrated on Figure 1, showed a significant BP decrease with age in all ROIs (hippocampus, parahippocampal gyrus, insula, anterior and posterior cingulate gyrus, orbitofrontal and frontal gyrus, temporal, parietal, and occipital lobes, and raphe nucleus), except in amygdala and temporal pole. Global BP values decreased significantly with age in the female population with a slope of 3.6% per decade and a mean reduction in ^{18}F-MPPF BP of 15% from 20 to 60 y.

Males. SPM analysis II revealed a significant BP decrease with age in small clusters of voxels located in the superior frontal gyrus and in the precuneus (Table 3). The inverse contrast showed a significant BP increase in the left middle frontal gyrus and in the rectus gyrus bilaterally (Fig. 2F).

The ROI analysis showed a significant positive linear correlation between age and BP in amygdala and temporal pole. Conversely, a significant negative linear correlation was found in the superior temporal gyri, in the opercular region, in the inferior and superior parietal cortices, and in the occipital lobe. Global BP values were not correlated with age (Fig. 1).

Evolution in ^{18}F-MPPF BP with Decades

From the ANOVA of ROI results, where decade of age and lateralization were considered as independent factors, we did not find any significant influence of the lateralization on regional BP values. Conversely, BP was primarily influenced by the age factor in a manner different for male and female groups.

Females. The statistical analysis of ROI data showed no influence of the decade of age on the variance in the temporal pole and in the inferior temporal, superior parietal, and occipital gyri. In the remaining regions, where the decade factor had a significant influence, the post hoc analysis revealed a significant decrease between subjects in their 20s and their 30s in amygdala, between subjects in their 40s and their 50s in amygdala and operculum, and between subjects

TABLE 1
^{18}F-MPPF BP in 18 Anatomic ROIs Determined with Data of 53 Subjects, Split by Decade of Age and Sex

Region	Decade: female				
	20s	30s	40s	50s	60s
Amygdala	0.74 ± 0.18	0.95 ± 0.12	0.82 ± 0.14	0.91 ± 0.17	0.70 ± 0.10
Hippocampus	1.24 ± 0.19	1.27 ± 0.07	1.16 ± 0.14	1.14 ± 0.16	0.96 ± 0.11
Parahippocampus	1.06 ± 0.23	1.06 ± 0.13	1.01 ± 0.08	0.98 ± 0.17	0.80 ± 0.09
Pole	0.96 ± 0.16	1.01 ± 0.13	0.99 ± 0.06	0.95 ± 0.11	0.86 ± 0.11
Insula	0.89 ± 0.18	0.91 ± 0.14	0.85 ± 0.08	0.73 ± 0.17	0.58 ± 0.12
Anterior cingulate	0.61 ± 0.16	0.65 ± 0.10	0.63 ± 0.07	0.60 ± 0.07	0.48 ± 0.11
Posterior cingulate	0.62 ± 0.16	0.56 ± 0.11	0.58 ± 0.07	0.51 ± 0.09	0.45 ± 0.10
Orbitofrontal	0.58 ± 0.13	0.58 ± 0.11	0.58 ± 0.07	0.54 ± 0.09	0.42 ± 0.09
Inferior temporal	0.68 ± 0.15	0.63 ± 0.10	0.66 ± 0.05	0.57 ± 0.13	0.54 ± 0.13
Middle temporal	0.71 ± 0.18	0.67 ± 0.10	0.67 ± 0.05	0.61 ± 0.12	0.51 ± 0.10
Superior temporal	0.71 ± 0.16	0.64 ± 0.11	0.63 ± 0.06	0.54 ± 0.11	0.43 ± 0.09
Opercule	0.56 ± 0.19	0.57 ± 0.12	0.57 ± 0.07	0.45 ± 0.11	0.35 ± 0.07
Inferior parietal	0.53 ± 0.15	0.50 ± 0.10	0.49 ± 0.04	0.44 ± 0.11	0.36 ± 0.09
Superior parietal	0.44 ± 0.16	0.38 ± 0.09	0.38 ± 0.07	0.36 ± 0.07	0.29 ± 0.08
Occipital	0.39 ± 0.13	0.39 ± 0.07	0.34 ± 0.05	0.35 ± 0.06	0.32 ± 0.07
Frontal	0.46 ± 0.15	0.46 ± 0.08	0.44 ± 0.03	0.42 ± 0.11	0.30 ± 0.08
Raphe nucleus	0.62 ± 0.16	0.56 ± 0.30	0.50 ± 0.10	0.45 ± 0.12	0.30 ± 0.10
Thalamus	0.01 ± 0.11	0.11 ± 0.17	0.07 ± 0.05	0.07 ± 0.10	0.01 ± 0.05
Global BP	0.66 ± 0.16	0.66 ± 0.09	0.63 ± 0.04	0.59 ± 0.11	0.49 ± 0.09
Region	Decade: male				
	20s	30s	40s	50s	60s
Amygdala	0.81 ± 0.16	0.76 ± 0.07	0.87 ± 0.14	0.87 ± 0.12	0.99 ± 0.15
Hippocampus	1.28 ± 0.12	1.03 ± 0.15	1.21 ± 0.15	1.17 ± 0.13	1.30 ± 0.10
Parahippocampus	1.03 ± 0.17	0.83 ± 0.09	0.95 ± 0.13	0.98 ± 0.09	1.02 ± 0.07
Pole	0.94 ± 0.08	0.85 ± 0.09	0.98 ± 0.15	0.99 ± 0.09	1.02 ± 0.22
Insula	0.91 ± 0.13	0.71 ± 0.10	0.83 ± 0.18	0.78 ± 0.13	0.74 ± 0.09
Anterior cingulate	0.68 ± 0.16	0.48 ± 0.07	0.58 ± 0.15	0.57 ± 0.09	0.62 ± 0.16
Posterior cingulate	0.69 ± 0.17	0.44 ± 0.07	0.53 ± 0.10	0.53 ± 0.09	0.60 ± 0.15
Orbitofrontal	0.56 ± 0.11	0.46 ± 0.05	0.58 ± 0.12	0.54 ± 0.07	0.63 ± 0.22
Inferior temporal	0.65 ± 0.09	0.55 ± 0.09	0.63 ± 0.10	0.63 ± 0.07	0.62 ± 0.14
Middle temporal	0.69 ± 0.11	0.54 ± 0.07	0.66 ± 0.14	0.65 ± 0.07	0.64 ± 0.15
Superior temporal	0.76 ± 0.09	0.54 ± 0.06	0.63 ± 0.14	0.61 ± 0.09	0.59 ± 0.13
Opercule	0.66 ± 0.16	0.46 ± 0.06	0.57 ± 0.14	0.51 ± 0.05	0.45 ± 0.10
Inferior parietal	0.64 ± 0.12	0.39 ± 0.06	0.49 ± 0.12	0.45 ± 0.05	0.45 ± 0.13
Superior parietal	0.55 ± 0.16	0.32 ± 0.07	0.38 ± 0.11	0.33 ± 0.07	0.30 ± 0.05
Occipital	0.51 ± 0.12	0.33 ± 0.06	0.41 ± 0.11	0.38 ± 0.05	0.35 ± 0.10
Frontal	0.53 ± 0.11	0.35 ± 0.05	0.44 ± 0.10	0.42 ± 0.05	0.39 ± 0.15
Raphe nucleus	0.51 ± 0.11	0.38 ± 0.16	0.52 ± 0.13	0.51 ± 0.21	0.43 ± 0.10
Thalamus	0.06 ± 0.11	−0.03 ± 0.07	0.03 ± 0.08	0.05 ± 0.05	0.04 ± 0.05
Global BP	0.70 ± 0.10	0.53 ± 0.04	0.63 ± 0.12	0.61 ± 0.06	0.63 ± 0.12

Data are presented as mean ± SD. Left and right are averaged.

in their 50s and their 60s in all ROIs (mean decrease of 17%) except the posterior cingulate, middle temporal, and opercular cortices.

The SPM analysis III (Table 4), revealed a significant BP decrease independent of global variations between subjects in their 40s and their 50s in the right superior temporal gyrus (Fig. 3A) and a significant BP increase between subjects in their 50s and their 60s in the left fusiform gyrus (Fig. 3B). Other comparisons did not show any significant clusters.

Males. The statistical analysis of ROI data showed a significant influence of decade of age on BP in all regions except in the raphe nucleus, and in the inferior temporal gyrus. In regions where the decade of age had a significant influence on variance, the post hoc analysis revealed (i) a significant BP decrease between the 20–29 and the 30–39 age group involving all ROIs except the amygdala and the temporal pole, and (ii) a significant BP increase between the 30–39 y and the 40–49 age group in all ROIs except in the cingulate, superior parietal and occipital gyri. No difference was found either between subjects in their 40s and 50s or between those in their 50s and 60s.

The SPM analysis III (Table 4) showed (i) a decrease in BP between the 20–29 y and 30–39 y age group in the

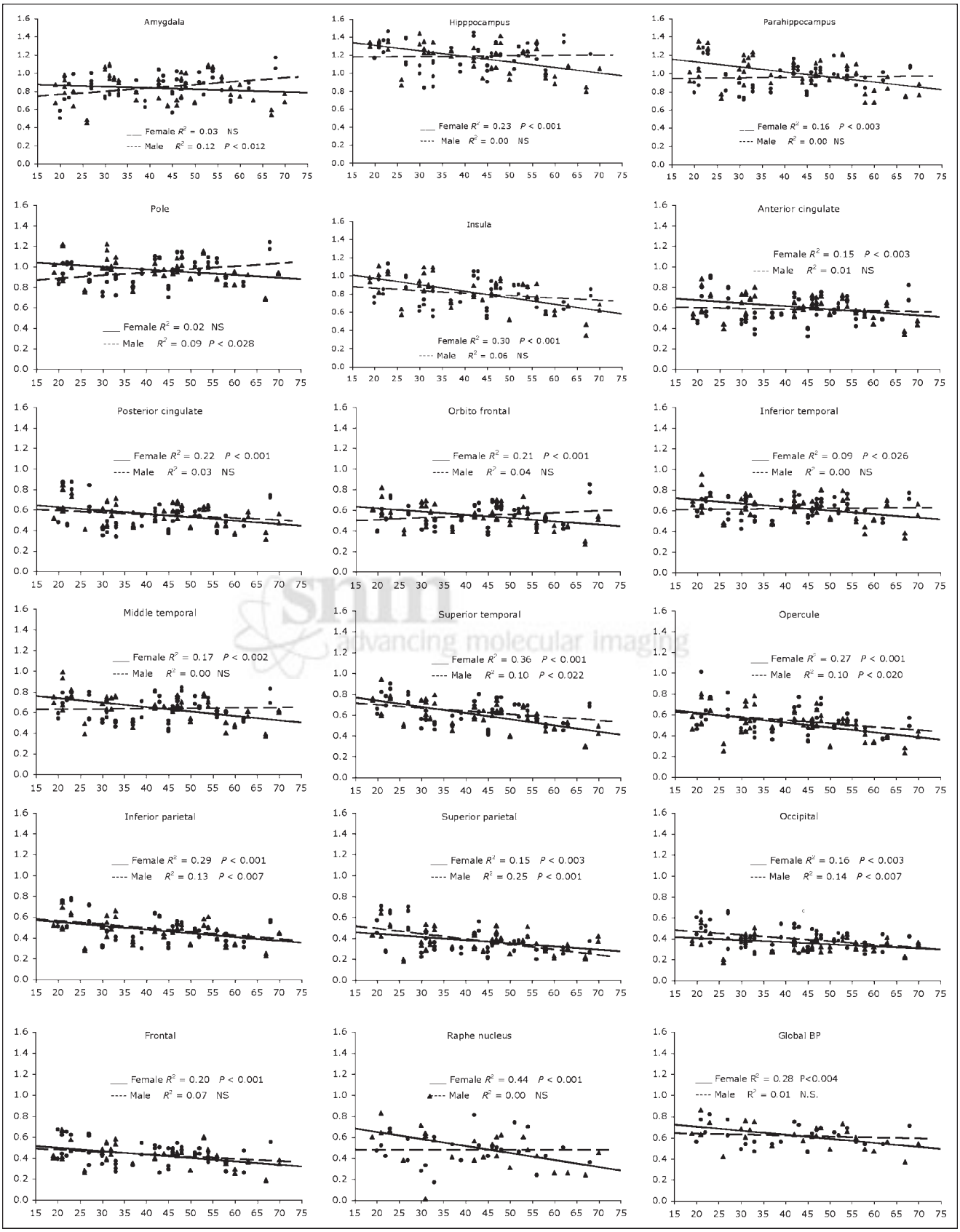

FIGURE 1. Scatter plot of BP values for 53 subjects in 18 anatomic ROIs manually delineated on individual MR images. Left and right values are not differentiated. Triangles are for female data, and dots are for male data. Linear regression curves are plotted for females (solid line) and for males (dashed line) independently. NS = not significant; R^2 = correlation coefficient.

TABLE 2
Analysis II: Sex Differences

Region	BA	Peak *z*-score	Extension *k*	Peak level P(*z*)<	Cluster level P(*z*, *k*)<	MNI coordinates *x*	*y*	*z*
Male binding superior to female								
R inferior parietal gyrus	7	5.20	240	0.002	0.011	36	−78	46
Female binding superior to male								
R middle temporal gyrus	21	4.59	318	0.032	0.003	66	−22	−12
R parahippocampal gyrus	36	4.55	1,572	0.038	0.001	34	−18	−20
R rectus gyrus	11	4.41	904	0.066	0.001	8	36	−20
L inferior temporal gyrus	20	4.21	431	0.134	0.001	−52	−12	−34
R precentral gyrus	4	4.03	259	0.238	0.080	40	−2	16
L anterior cingulate gyrus	31	4.02	240	0.247	0.011	−8	−64	24
R temporal pole	20	3.92	214	0.328	0.017	28	4	−38
R superior frontal gyrus	10	3.92	267	0.329	0.007	10	56	18
L hippocampus		3.86	202	0.394	0.021	−32	−34	−10

BA = Brodmann's area.

SPM result of analysis II (linear regression of age on BP, with a sex group factor). Results of *t* contrast of sex group comparison, independently of age effect. Cluster selection is based on corrected probability of the peak ($P < 0.05$) or corrected probability of the cluster size ($P < 0.05$). Clusters are formed by connected voxels with an individual uncorrected probability of 0.001. Region: L = left; R = right. Peak *z*-score: *z*-score of the maximum of the cluster (Student *t* transformed to *z*-score). Extension *k*: size of the cluster in number of suprathreshold (uncorrected $P < 0.001$) connected voxels. Peak level: corrected probability of the peak. Cluster level: joint corrected probability of the cluster extension and peak *z*-score. MNI coordinates: coordinates of the peak in the MNI templates with the Talairach referential.

inferior parietal gyrus and precuneus bilaterally, in the left cingulate gyrus (Fig. 3C), in the left supplementary motor area, in the medial and lateral superior frontal gyrus (Fig. 3D), and (ii) an increase in BP between the 30–39 and the 40–49 age group in the right middle frontal gyrus (Fig. 3E), and left superior frontal gyrus (Fig. 3F).

DISCUSSION

Use of a Large Database

To our knowledge, this study is the first report exploring 5-HT_{1A} receptor binding with ^{18}F-MPPF in a large population including both male and female subjects. Previous PET studies have used another antagonist of 5-HT_{1A}, ^{11}C-WAY100635, in either smaller populations (n = <25) (*19–21*) or in a large group of only male volunteers (n = 61) (*13*). Our database is large enough to perform statistical inference of ^{18}F-MPPF binding modifications to 5-HT_{1A} receptors in the context of pathologies or specific cerebral functions involving the serotoninergic system, or to study the effect of drugs on the serotoninergic system. Accordingly, as patients began to be compared with control populations, we could assess significant bilateral abnormalities in ^{18}F-MPPF binding to 5-HT_{1A} receptors using our database in epileptic patients with temporal lobe epilepsy (*15,16*).

Moreover, the large sampling of female and male subjects over aging permits the study of pathologies such as depression, Alzheimer' disease, or anorexia, which may differentially affect men versus women or younger versus older patients.

This study continues our previous work (*10*) in which we quantified a whole set of ^{18}F-MPPF transport, binding, and metabolization parameters. This quantification implied arterial blood sampling and a multiple injection protocol, which was not appropriate for large-scale studies and justified the use of a simplified protocol. In the present work, the SRTM, with the cerebellum as reference, provides 3 parameters related to binding (BP), washout (k_2), and delivery (R_1) with sufficient stability to be computed as parametric images suitable for statistical voxel-by-voxel analysis. Furthermore, from our spatially normalized static PET images we were able to create a ^{18}F-MPPF template in the MNI stereotactic space, which allows future spatial normalization procedures in the absence of individual anatomic MR images.

Methodologic Issues

A limitation in our database is the small number of subjects included in the 60–69 y-old age group. Indeed, the different size of our population samples impairs the statistical power for the detection of specific differences between each group and might have an impact on our results. However, SDs for males and females in their 60s were of similar magnitude as for other age groups (Table 1). Nevertheless, to obtain a direct-paired comparison of parametric data between patients of the 60s decade (like patients with Alzheimer's disease) and controls, additional healthy volunteers of this age group should be included.

Another methodologic issue relates to the drawing of ROIs that were manually traced directly on the individual

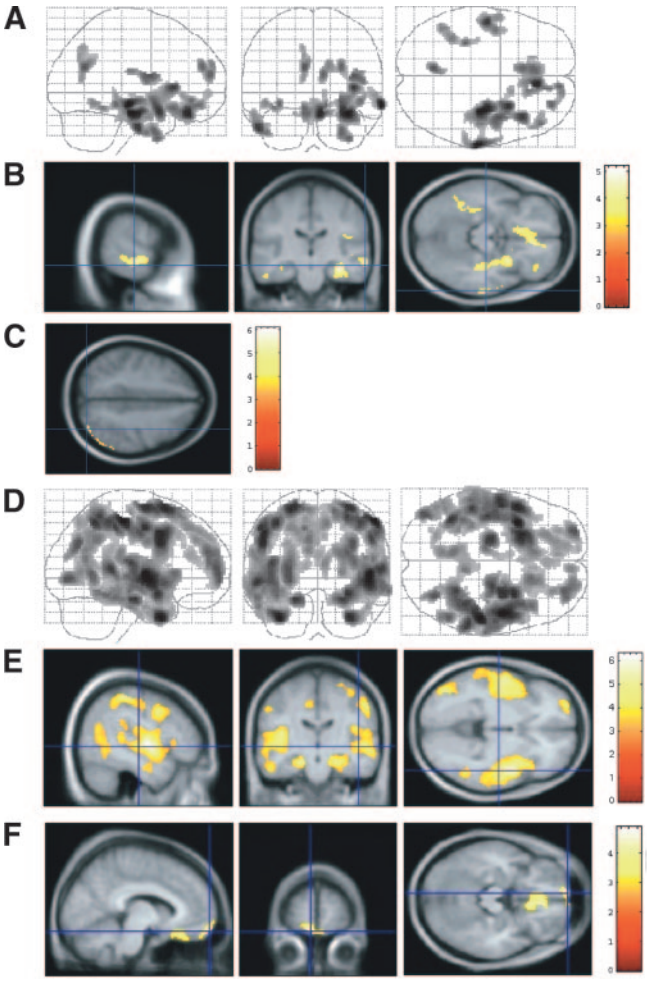

FIGURE 2. SPM of ^{18}F-MPPF binding with age and sex effect (analysis II). (A and B) Increase in ^{18}F-MPPF binding in female compared with male subjects independently of age effect. (A) Maximum intensity projection (MIP) in the *x*-, *y*-, and *z*-directions of the statistical map. *t* score threshold $P < 0.001$ uncorrected for multiple comparisons; cluster threshold $P < 0.05$ corrected for multiple comparisons. Right of the brain is the right of the figure. (B) Three orthogonal views ($x, y, z = 66, -22, -14$) of SPM centered on peak situated in right middle temporal gyrus (Boadmann's area [BA] 21) superimposed on averaged normalized MR images from 23 female subjects. Right hippocampus is visible on right hemisphere in transverse and coronal views. (C) Binding of ^{18}F-MPPF increase in male vs. female independent of age effect. Transverse view of SPM shows a side effect in surface of parietal cortex ($x, y, z = 36, -78, 46$). (D and E) Negative linear correlation of BP with age in female subjects. (D) MIP of statistical map. *t* score's threshold $P < 0.001$ uncorrected for multiple comparisons; cluster threshold $P < 0.05$ corrected for multiple comparisons. (E) Three orthogonal views of SPM centered on peak situated in right superior temporal gyrus ($x, y, z = 48, -19, -5$; BA 22) superimposed on averaged normalized MR images from 23 female subjects. (F) Positive linear correlation of BP with age in male population. Three orthogonal views of SPM (*t* threshold $P < 0.001$ uncorrected; cluster threshold $P < 0.05$ corrected, $x, y, z = -8, 64, -18$) centered on peak situated in left middle frontal gyrus (BA 11) superimposed on averaged normalized MR images from 22 male subjects. Rectus gyrus is visible on sagittal and transverse views.

MR images. The uncertainty of the delineation in the cortical and subcortical regions is not suspected. The problem might be located in the raphe nucleus. Given that this structure is not really a nucleus in the cytoarchitectural sense of the term, a delineation should be arbitrarily chosen either on a fixed volume embedding the raphe in the brainstem with an a priori knowledge of its position or with an arbitrary delineation based on the ^{18}F-MPPF activity threshold from a static equilibrium ^{18}F-MPPF image. We chose this second approach, fixing a threshold at 80% of the local maximum activity located in the brainstem. However, this delineation would not be suitable in patients presenting a severely decreased ^{18}F-MPPF binding in the raphe nucleus. In such cases, a parametric image without a priori delineation of the raphe would be more appropriate.

The question of volume delineation of structure contributes to the complication of the PVE and spillover due to the limited resolution of the PET scanner. The correction method based on geometric matrix transfer (*22*) can be applied. In this study we considered uncorrected results, yet we verified that the variation of volume over subjects could not explain the variation of BP. As in Tauscher et al. (*21*), we found that ROI volumes were not correlated with BP changes except in 2 regions—that is, the insula in women and the raphe nucleus in men. However, in these 2 regions, linear regression revealed a negative correlation between volume and BP. Therefore, the hypothesis that BP reductions were attributed to a PVE induced by ROI volume reduction was ruled out. This does not mean that no PVE affected our measures but that PVE cannot explain BP reduction in our study.

Sex Difference in ^{18}F-MPPF Binding

Sex differences are observed in several serotonin-regulated behaviors (sexual, aggression) or mental disorders (eating disorders, anxiety disorders, depression). As an example, the rate of mood disorders was shown to be almost double in females versus that in males (*23*).

To our knowledge, only 2 PET studies explored male/females differences in 5-HT$_{1A}$ binding using ^{11}C-WAY100635 (*20,21*). Parsey et al. (*20*) found higher values of distribution volume in specific compartments (V3) for women compared with men. When considering the SRTM BP (i.e., V3 normalized to the nonspecific distribution volume), this sex effect disappeared as in Tauscher et al. (*21*). In our study, where BP was calculated with the SRTM, the 2-sample *t* test comparing parametric images of BP in male versus female groups consistently did not show any significant difference. However, once the effect of age had been removed by an ANCOVA, significantly higher BP values in females than in males were shown in limbic, paralimbic, and frontal regions, areas known to be particularly rich in 5-HT$_{1A}$ receptors. It is noteworthy that Tauscher et al. found a "sex × age" interaction in some regions, but that did not survive a correction for multiple comparisons. In our study,

TABLE 3
Analysis II: Linear Correlation

Region	BA	Peak *z*-score	Extension *k*	Peak level P(*z*)<	Cluster level P(*z*, *k*)<	MNI coordinates *x*	*y*	*z*
Female: linear increase with age								
None								
Female: linear decrease with age								
R superior temporal gyrus	22	5.35	8,988	0.001	0.001	48	−6	2
L temporal pole	38	5.25	10,016	0.002	0.001	−36	8	−36
L superior temporal gyrus	6	4.98	4,137	0.006	0.001	−24	12	64
R parahippocampal gyrus	36	4.69	436	0.021	0.001	24	−16	−20
R middle temporal gyrus	21	4.43	573	0.060	0.001	52	−56	4
L middle frontal gyrus	6	4.22	204	0.131	0.020	−12	−22	46
R anterior cingulate gyrus	32	3.61	174	0.671	0.035	2	36	20
L anterior cingulate gyrus	24	3.58	190	0.696	0.026	−2	14	34
Male: linear increase with age								
L middle frontal gyrus	11	4.37	211	0.076	0.018	−8	64	−18
R rectus gyrus	11	4.34	676	0.085	0.001	6	22	−22
Male: linear decrease with age								
R precuneus	7	5.33	161	0.021	0.044	36	−74	52
L superior frontal gyrus		4.48	365	0.210	0.002	−18	28	62

BA = Brodmann's area.

SPM result of analysis II (linear regression of age on BP, with a sex group factor). Results of *t* contrasts of linear regression in female group and in male group. See legend of Table 2 for cluster selection and column definitions.

statistical differences between women and men are more likely to be attributed to a higher sensitivity resulting from a larger number of subjects (about twice as in Tauscher et al. or Parsey et al. (*20*)) or to the different properties of ^{18}F-MPPF versus ^{11}C-WAY100635 relative to 5-HT_{1A} receptors.

The higher BP values found in women can be interpreted as a higher density of 5-HT_{1A} receptors in women

TABLE 4
Analysis III: Decade Difference

Region	BA	Peak *z*-score	Extension *k*	Peak level P(*z*)<	Cluster level P(*z*, *k*)<	MNI coordinates *x*	*y*	*z*
Female 40s to 50s decrease								
Temporal superior gyrus	12	4.29	185	0.385	0.025	54	6	−8
Female 50s to 60s increase								
Fusiform gyrus	39	4.82	128	0.014	0.077	−44	−70	20
Male 20s to 30s decrease								
L inferior parietal gyrus	40	4.71	2,039	0.022	0.001	−46	−40	44
R inferior parietal gyrus	40	4.49	331	0.052	0.002	54	−48	46
R inferior parietal gyrus	39	4.02	424	0.259	0.001	54	−64	26
L middle frontal gyrus	10	3.97	528	0.304	0.001	−40	48	12
L superior frontal gyrus	8	3.82	713	0.453	0.001	−14	32	58
L posterior cingulate gyrus	32	3.69	153	0.596	0.047	−10	−6	44
Male 30s to 40s increase								
R middle frontal gyrus	9	3.70	257	0.584	0.007	6	34	−12
L middle frontal gyrus	9	3.56	166	0.744	0.036	−30	44	32

BA = Brodmann's area.

SPM result of analysis III (ANOVA with sex and decade of age group factors). Results of *t* contrast between decade of age in female groups and in male groups from their 20s to their 60s. See legend of Table 2 for cluster selection and column definitions. Only contrasts showing significant results are listed.

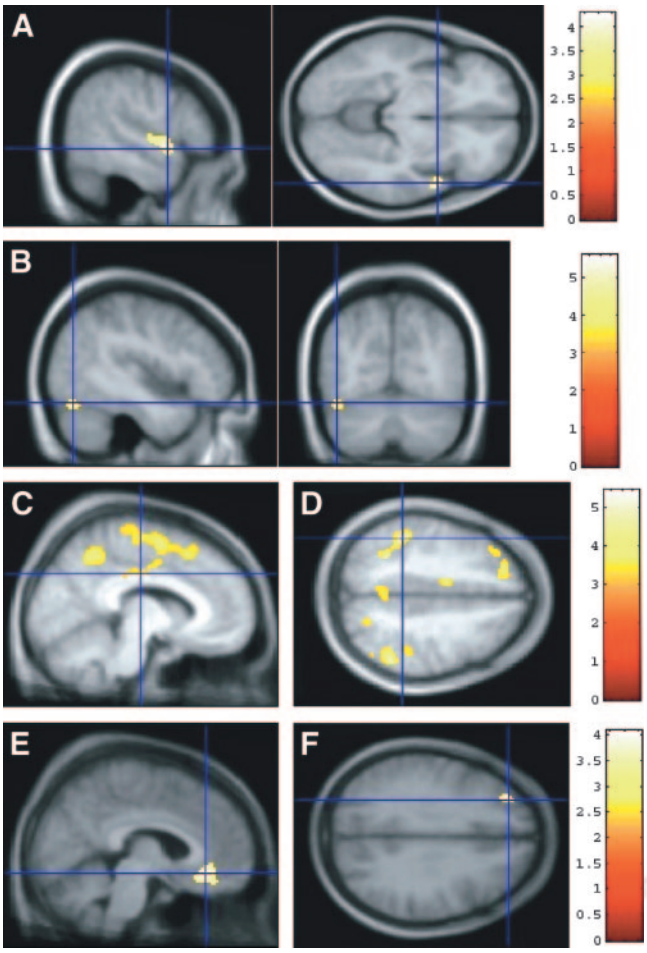

FIGURE 3. SPM of ^{18}F-MPPF binding by decade of age (analysis III). (A and B) SPM of differences between decades in female population. (A) Decrease in ^{18}F-MPPF binding between subjects in their 40s and their 50s in right superior temporal gyrus (sagittal view, $x = 54$ mm; transverse view, $z = -8$ mm). (B) Increase in ^{18}F-MPPF binding from 50s to 60s decades of age in left fusiform gyrus (sagittal view, $x = -44$ mm; coronal view, $y = -70$ mm). (C and D) SPM of differences between decade of age in male population: decrease in ^{18}F-MPPF binding between subjects in their 20s and 30s. (C) Sagittal view ($x = -10$ mm): Decrease in left posterior cingulate gyrus (cross), superior parietal lobule, and superior frontal gyrus. (D) Transverse view ($z = +44$ mm), decrease in left inferior parietal lobule (cross). BP values appear symmetric in right inferior parietal, left posterior cingulate, and left middle frontal cortex. (E and F) SPM of differences between decades in female population: Increase in ^{18}F-MPPF binding between subjects in their 30s and 40s. (E) Sagittal view ($x = +6$ mm), right middle frontal gyrus (BA 9). (F) Transverse view ($z = 32$ mm), left middle frontal gyrus.

compared with men; on the other hand, given that ^{18}F-MPPF is sensitive to endogenous variations of 5-HT concentration (*24*), higher BP values in women could also be interpreted as a higher availability of 5-HT$_{1A}$ receptor sites due to a lower concentration of 5-HT. BP variations could also be interpreted as a K_d variation of ^{18}F-MPPF binding to 5-HT$_{1A}$. However, 5-HT synthesis has not yet been assessed in vivo in male and female subjects, and, in addition, postmortem studies in humans using 8-hydroxy-2-(di-*n*-propylamino)tetralin failed to find any sex effect on B_{max} (*25,26*).

Variation of BP with Age

In our study, we showed that aging influenced the BP values in our healthy subjects. This is an expected result as normal aging leads to changes in most neurotransmission systems as a consequence of presynaptic reduction of the neurotransmitter (which could be due to neuronal loss, decrease in synthesis, or increase of metabolism degradation), decrease in the density of postsynaptic receptors, or deficiency in signal transduction mechanisms. Although some studies in humans fail to find any effect of aging on 5-HT$_{1A}$ receptor binding in healthy subjects (*27*), other postmortem studies in humans (*26*) show a substantial reduction of binding with age (up to 50%) attributed to a decrease in receptor density with no change in affinity (*26*). These studies, however, do not provide any information on sex.

Our results revealed a sex-specific effect of age on BP. We found a linear decrease of BP with age in almost all regions in women. In men, changes in BP were region specific with no correlation between BP and age in most limbic and paralimbic regions, with either an increase or a decrease of BP with age in the remaining regions. Among PET studies using ^{11}C-WAY100635 to explore the linear relation between age and BP, the results are contradictory. Some studies found a BP decrease with age but no effect of sex (*21*) or a BP decrease in men but not in women (*19*) or no correlation between BP in men (*13,28*) or in men and women (*20*). These results, along with ours, most likely reflect differences in population sizes, age range (oldest subjects, 55–80 y), camera field of view, or affinity of the radioligand for 5-HT$_{1A}$ receptors.

However, using comparable methodologies, postmortem studies in humans also give inconsistent results. Although Matsubara et al. (*29*) found a negative correlation between the 5-HT$_{1A}$ receptor density (B_{max}) and age in male but not in female controls, Palego et al. (*25*) described both significant increases and decreases of B_{max} with age in women, whereas men showed a decrease of affinity with age in the occipital regions.

Analysis of BP changes by decade of age adds to the understanding of the results regarding the linear changes with age. This analysis reveals specific patterns of BP changes over the decade of age. In women, our data suggest that there is a widespread decrease of BP with age, which worsens after 50 y. In men, the analysis by decade reveals that BP decreases between 20 and 30 y but that this decrease in compensated by an increase between 30 and 40 y for almost all regions. This would explain the absence of a linear correlation between age and BP in men. Interestingly, the SPM analysis shows that the decrease between 20 and 30 y is even more significant in the parietal, frontal, and precuneus regions, which are precisely the areas were a

linear negative correlation between BP and age was identified. These specific patterns of BP changes with age in men are difficult to interpret, primarily as linear changes would be expected as a consequence of neuronal loss during aging. Unfortunately, the only study reporting such specific patterns of BP changes over the decade of age (*30*) explored 5-HT_{2A} receptors and pooled the results from male and female subjects. Interestingly, however, on the comparison of these data with those of Palego et al. (*25*) and Dillon et al. (*26*), the authors suggested that aging effects on the serotoninergic system seem to depend on age groups and that the decrease in 5-HT_{1A} receptor density is more pronounced in younger men and older women. Whether regulation processes occur in men during midlife is difficult to state from our data but might explain differences in the incidence of psychiatric or anxiety disorders in older male and female subjects.

CONCLUSION

Our data revealed that ^{18}F-MPPF binding to 5-HT_{1A} receptors is different in men and women independently of age and that changes of BP with age are sex specific, which corroborates the different epidemiology of psychiatric diseases in elderly. Our results justify the use of a large normative database to eliminate age and sex effects from the statistical analysis of parameters of interest in the study of patient populations with PET and ^{18}F-MPPF.

ACKNOWLEDGMENTS

The authors thank the entire medical and radiochemistry staff of the CERMEP for their technical and human assistance. The authors thank Professor Jean-François Pujol for the initiative and his support to this research.

REFERENCES

1. Barnes NM, Sharp T. A review of central 5-HT receptors and their function. *Neuropharmacology.* 1999;38:1083–1152.
2. Cliffe IA. A retrospect on the discovery of WAY-100635 and the prospect for improved 5-HT_{1A} receptor PET radioligands. *Nucl Med Biol.* 2000;27:441–447.
3. Pike VW, McCarron JA, Lammertsma AA, et al. Exquisite delineation of 5-HT1A receptors in human brain with PET and [carbonyl-^{11}C]WAY-100635. *Eur J Pharmacol.* 1996;301:R5–R7.
4. Farde L, Ito H, Swahn CG, Pike VW, Halldin C. Quantitative analyses of carbonyl-carbon-11-WAY-100635 binding to central 5-hydroxytryptamine-1A receptors in man. *J Nucl Med.* 1998;39:1965–1971.
5. Le Bars D, Lemaire C, Ginovart N, et al. High-yield radiosynthesis and preliminary in vivo evaluation of p-[^{18}F]MPPF, a fluoro analog of WAY-100635. *Nucl Med Biol.* 1998;25:343–350.
6. Zhuang ZP, Kung MP, Chumpradit S, Mu M, Kung HF. Derivatives of 4-(2′-methoxyphenyl)-1-[2′-(N-2″-pyridinyl-p-iodobenzamido)ethyl]piperazine (p-MPPI) as 5-HT1A ligands. *J Med Chem.* 1994;37:4572–4575.
7. Plenevaux A, Weissmann D, Aerts J, et al. Tissue distribution, autoradiography, and metabolism of 4-(2′-methoxyphenyl)-1-[2′-[N-2″-pyridinyl)-p- [^{18}F]fluorobenzamido]ethyl]piperazine (p-[^{18}F]MPPF), a new serotonin 5-HT_{1A} antagonist for positron emission tomography: an in vivo study in rats. *J Neurochem.* 2000;75:803–811.
8. Ginovart N, Hassoun W, Le Bars D, Weissmann D, Leviel V. In vivo characterization of p-[^{18}F]MPPF, a fluoro analog of WAY-100635 for visualization of 5-HT_{1a} receptors. *Synapse.* 2000;35:192–200.
9. Passchier J, van Waarde A, Pieterman RM, et al. Quantitative imaging of 5-HT_{1A} receptor binding in healthy volunteers with [^{18}F]p-MPPF. *Nucl Med Biol.* 2000; 27:473–476.
10. Costes N, Merlet I, Zimmer L, et al. Modeling [^{18}F]MPPF PET kinetics for the determination of 5-HT1A concentration with multi-injection. *J Cereb Blood Flow Metab.* 2002;22:753–763.
11. Gunn RN, Lammertsma AA, Grasby PM. Quantitative analysis of [carbonyl-^{11}C]WAY-100635 PET studies. *Nucl Med Biol.* 2000;27:477–482.
12. Parsey RV, Slifstein M, Hwang DR, et al. Validation and reproducibility of measurement of 5-HT1A receptor parameters with [carbonyl-^{11}C]WAY-100635 in humans: comparison of arterial and reference tissue input functions. *J Cereb Blood Flow Metab.* 2000;20:1111–1133.
13. Rabiner EA, Messa C, Sargent PA, et al. A database of [^{11}C]WAY-100635 binding to 5-HT_{1A} receptors in normal male volunteers: normative data and relationship to methodological, demographic, physiological, and behavioral variables. *Neuroimage.* 2002;15:620–632.
14. Goldberg DP, Hillier VF. A scaled version of the general health questionnaire. *Psychol Med.* 1979;9:139–145.
15. Merlet I, Ostrowsky K, Costes N, et al. 5-HT1A receptor binding and intracerebral activity in temporal lobe epilepsy: an [^{18}F]MPPF PET study. *Brain.* 2004; 127:900–913.
16. Merlet I, Ryvlin P, Costes N, et al. Statistical parametric mapping of 5-HT1A receptor binding in temporal lobe epilepsy with hippocampal ictal onset on intracranial EEG. *Neuroimage.* 2004;22:886–896.
17. Gunn RN, Lammertsma AA, Hume SP, Cunningham VJ. Parametric imaging of ligand-receptor binding in PET using a simplified reference region model. *Neuroimage.* 1997;6:279–287.
18. Poline JB, Worsley KJ, Evans AC, Friston KJ. Combining spatial extent and peak intensity to test for activations in functional imaging. *Neuroimage.* 1997;5:83–96.
19. Meltzer CC, Drevets WC, Price JC, et al. Gender-specific aging effects on the serotonin 1A receptor. *Brain Res.* 2001;895:9–17.
20. Parsey RV, Oquendo MA, Simpson NR, et al. Effects of sex, age, and aggressive traits in man on brain serotonin 5-HT1A receptor binding potential measured by PET using [C-11]WAY-100635. *Brain Res.* 2002;954:173–182.
21. Tauscher J, Verhoeff NP, Christensen BK, et al. Serotonin 5-HT1A receptor binding potential declines with age as measured by [^{11}C]WAY-100635 and PET. *Neuropsychopharmacology.* 2001;24:522–530.
22. Rousset OG, Ma Y, Evans AC. Correction for partial volume effects in PET: principle and validation. *J Nucl Med.* 1998;39:904–911.
23. Oquendo MA, Ellis SP, Greenwald S, Malone KM, Weissman MM, Mann JJ. Ethnic and sex differences in suicide rates relative to major depression in the United States. *Am J Psychiatry.* 2001;158:1652–1658.
24. Zimmer L, Mauger G, Le Bars D, Bonmarchand G, Luxen A, Pujol JF. Effect of endogenous serotonin on the binding of the 5-HT1A PET ligand ^{18}F-MPPF in the rat hippocampus: kinetic beta measurements combined with microdialysis. *J Neurochem.* 2002;80:278–286.
25. Palego L, Marazziti D, Rossi A, et al. Apparent absence of aging and gender effects on serotonin 1A receptors in human neocortex and hippocampus. *Brain Res.* 1997;758:26–32.
26. Dillon KA, Gross-Isseroff R, Israeli M, Biegon A. Autoradiographic analysis of serotonin 5-HT1A receptor binding in the human brain postmortem: effects of age and alcohol. *Brain Res.* 1991;554:56–64.
27. Lowther S, De Paermentier F, Cheetham SC, Crompton MR, Katona CL, Horton RW. 5-HT1A receptor binding sites in post-mortem brain samples from depressed suicides and controls. *J Affect Disord.* 1997;42:199–207.
28. Sargent PA, Kjaer KH, Bench CJ, et al. Brain serotonin1A receptor binding measured by positron emission tomography with [^{11}C]WAY-100635: effects of depression and antidepressant treatment. *Arch Gen Psychiatry.* 2000;57:174–180.
29. Matsubara S, Arora RC, Meltzer HY. Serotonergic measures in suicide brain: 5-HT1A binding sites in frontal cortex of suicide victims. *J Neural Transm Gen Sect.* 1991;85:181–194.
30. Gross-Isseroff R, Salama D, Israeli M, Biegon A. Autoradiographic analysis of age-dependent changes in serotonin 5-HT2 receptors of the human brain postmortem. *Brain Res.* 1990;519:223–227.